

# A Thermochemical Route to the Sustainable Upgrade of Plastic Solid Waste using Iron as a Catalyst Precursor

Letizia Marchetti<sup>a,\*</sup>, Cristiano Nicolella<sup>a</sup>, Leonardo Tognotti<sup>a</sup>, Szymon Doszczeczko<sup>b</sup>, Roberto Volpe<sup>b</sup>

<sup>a</sup>Dipartimento di Ingegneria Civile e Industriale, Università di Pisa, Largo Lucio Lazzarino 2, 56122, Pisa (PI), Italy

<sup>b</sup>School of Engineering and Material Science, Queen Mary University of London, Mile End Road, London, E1 4NS, UK

[letizia.marchetti@unipi.it](mailto:letizia.marchetti@unipi.it)

The management of plastic solid waste represents a significant challenge due to the rapid growth in plastic production and its inherent non-biodegradable nature. Pyrolysis appears as a promising alternative to landfilling and incineration, consisting of a thermal decomposition of feedstock in a sub-stoichiometric-oxygen environment, thus giving rise to three phases: a solid one (pyro-char), liquid, and gas. Although most works focus on optimizing (e.g. maximizing the yield or improving the quality of) the liquid and gaseous fractions, the pyro-char has not been given sufficient attention, despite its potential application in numerous desirable fields. The addition of transition metals such as Fe to feedstock prior to pyrolysis is interesting as it may contribute to an increase in yield and quality of the derived liquid and gaseous products while also improving the chemical characteristics of pyro-char towards higher added value applications such as heterogeneous catalysis. This experimental work investigates the effects of adding iron acetate to plastic solid waste prior to their pyrolysis and its role in the final properties of the produced pyro-char. Pyrolysis of four samples with different concentrations of iron acetate (0, 5, 10, and 20 % w/w dry basis) was carried at 25 °C min<sup>-1</sup> heating rate to 600 °C holding temperature for 2 hours. Analyses of the resulting pyro-char have shown that adding iron acetate considerably increases pyro-char yield, especially at 20 % concentration (yielding 14 % weight of pyro-char/weight of original feedstock). Iron becomes more concentrated in the resulting solid and its presence opens possibilities to potential use of pyro-chars as inexpensive catalysts for gas phase reactions such as (for example) the Reverse water-gas shift reaction.

## 1. Introduction

The management of plastic solid waste (PSW) has become a significant challenge as a result of the ongoing rise in plastic production and its inherent non-biodegradable nature (Taghavi et al., 2021). Among the various available methods, pyrolysis has been identified as a viable and effective route to upgrade PSW by producing solid, liquid and gaseous hydrocarbons. Such approach provides an alternative to landfill disposal thereby reducing environmental pollution. The aforementioned hydrocarbons resulting from the thermochemical process may serve as chemical scaffolds for further upgrade or as energy vectors, thereby contributing to the principles of a circular economy in the production and use of plastics. Pyrolysis has some environmental advantages over other processes for the treatment of PSW, primarily because it takes place in an environment which is poor in oxygen, thereby limiting the formation of dioxins and significantly reducing carbon monoxide and carbon dioxide emissions in the atmosphere (Al-Salem et al., 2017). While the results of experimental studies on the pyrolysis of plastics have been widely reported, most of those works focus on improving the yield and quality of the produced liquids and gases (Akhtar and Saidina Amin, 2012; Marchetti et al., 2024), while pyro-char, has often been overlooked. By contrast, studies on pyro-char produced from biomass pyrolysis (bio-chars) are much more frequent and the results of such studies may inspire routes to the pyrolysis upgrade of PSW. For example, Monlau et al. (2016) investigated the use of bio-chars, derived from a mix of goats, olive oil cake, triticale silage, and chicken manure, feedstock as a soil amendment. Similarly, Malik et al. (2023) have proposed a method for the synthesis of carbon-encapsulated iron nanoparticles via the pyrolysis of sporopollenin exine capsules of

*Lycopodium clavatum*. However, similarly to biomass, the intrinsically high physical and chemical heterogeneity of PSW poses non-trivial challenges when reproducibility and homogeneity of the resulting products are desired. The PSW, indeed, is usually characterized by the presence of different polymers and metals. The metals can play different roles during the pyrolysis process. Among them, iron emerges as it plays a significant role in enhancing the cracking of biomass pyrolysis vapors, thereby increasing the yield and quality of chars and concentration of hydrogen in the produced gases (Xia et al., 2023). Moreover, iron is one of the most promising owing to its abundance and cost-effectiveness (Kylar mack, 2023). In this study we concentrate on a characterization of the pyro-char to help identifying correlations between the pre-impregnation of PSW with different amounts of iron (II) acetate ( $\text{Fe}(\text{OAc})_2$ ) and the yield and surface properties of its derived pyrolyzed solid. The morphology of the pyro-char was also investigated *via* Scanning Electron Microscopy (SEM) and Energy Dispersive Spectroscopy (EDS).

## 2. Materials and Methods

The raw material used in this research is PSW classified under the EWC150106 code according to the European Waste Catalogue. This is a waste from the industrial production of densified polyolefins. The quantification of metal present in the raw feedstock were quantified *via* inductively coupled plasma optical emission spectrometry (ICP-OES) following standards UNI EN 13657:2004 and UNI EN ISO 11885:2009. Prior to pyrolysis, the dried PSW was impregnated with  $\text{Fe}(\text{OAc})_2$  using 0, 5, 10, and 20 %, where the concentration is evaluated as the weight of  $\text{Fe}(\text{OAc})_2$  on the weight of  $\text{PSW}+\text{Fe}(\text{OAc})_2$ . Approximately 0, 0.1, 0.2, and 0.5 g of  $\text{Fe}(\text{OAc})_2$  were dissolved in 40 mL of methanol, and a weighted amount of PSW (2 g) was added to give the desired concentrations. The mix was then stirred at 300 rpm for 2 hours at room temperature, then dried in air at 60 °C for 24 hours.

The prepared samples were pyrolyzed, as shown in Figure 1, in a single zone SafTherm® electric tube furnace (model STF1200-1Z) to 600°C peak temperature, 25°C/min heating rate in a 1 L/min nitrogen flow rate and 2 hours holding time at peak temperature. For each test, approximately 500 mg of sample were loaded in a covered ceramic crucible (5 mL) placed in a 6 cm diameter, 80 cm long quartz tube. Prior to the pyrolysis ramp, samples were purged in the nitrogen flow for 10 minutes and then kept at 105°C for an additional 10 minutes to ensure removal of any residual moisture. After pyrolysis, pyro-chars were collected, weighted, and stored in a desiccator for further analysis.

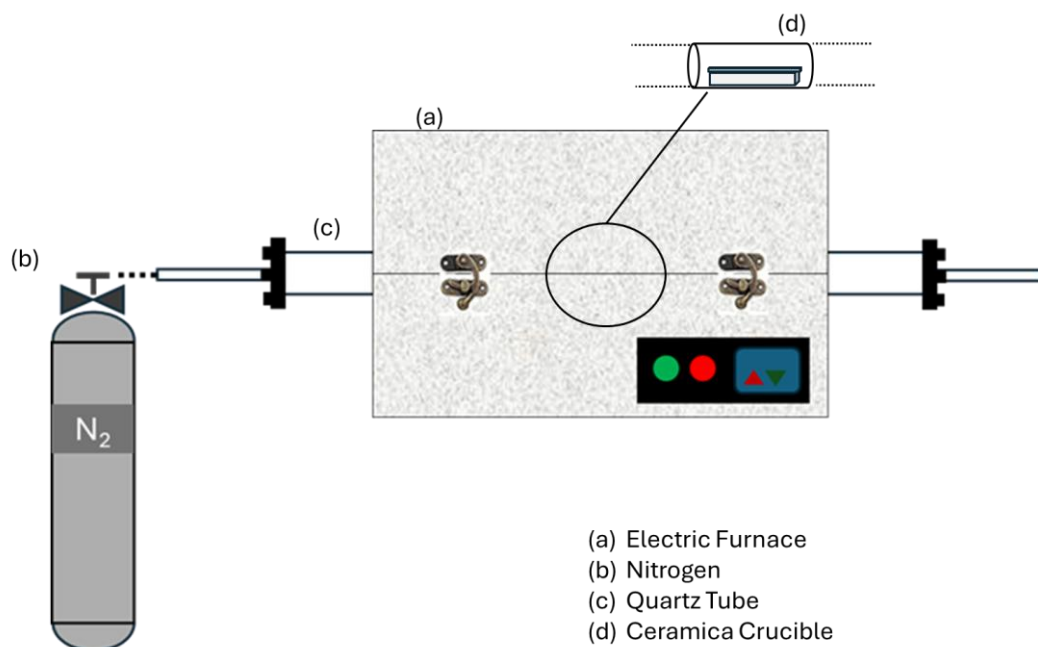


Figure 1: Scheme of the experimental batch lab-scale setup.

Pyro-chars surface morphology was studied in a field emission SEM (FE-SEM, FEI Inspect F50) at an acceleration voltage of 10 kV and a spot size of 3. The Elemental composition of the pyro-char obtained from a 20 % iron acetate impregnated sample, was obtained *via* EDS in the same instrument.

### 3. Results and Discussion

The metals present in the sample and their respective concentrations are reported in Table 1.

Table 1: Metallic composition of the raw PSW.

Metal	Unit	Value
Chlorine (Cl)	% w/w	2.1
Sulphur (S)	% w/w	<0.1
Iron (Fe)	mg/kg	55
Aluminium (Al)	mg/kg	50 300
Barium (Ba)	mg/kg	440
Calcium (Ca)	mg/kg	42 300
Chromium (Cr)	mg/kg	23
Magnesium (Mg)	mg/kg	1 300
Manganese (Mn)	mg/kg	260
Nickel (Ni)	mg/kg	<20
Lead (Pb)	mg/kg	200
Copper (Cu)	mg/kg	65
Tin (Sn)	mg/kg	<100
Zinc (Zn)	mg/kg	<350

The presence of metal, even in traces, is important for the complex thermochemical pathways occurring during pyrolysis, ultimately affecting the properties of derived pyro-chars (Collard et al., 2012). Our analyses revealed significant concentrations of iron, chlorine, aluminium, barium, calcium, magnesium, manganese and lead. Chlorine, typically from PVC, is a key element as it is responsible for the release of hydrochloric acid (HCl) during pyrolysis, which can damage pyrolyzers or processes downstream the pyrolysis (Alanazi et al., 2017). Conversely, the presence of elements like iron is often used as flame retardants and smoke suppressants during the combustion of PVC (Ji et al., 2020). The studies concentrations in iron acetate yielded the results presented in Figure 2.

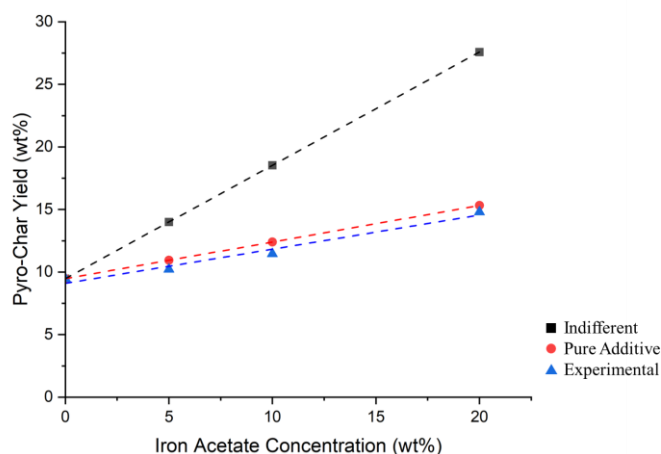


Figure 2: Pyro-char yields at different  $\text{Fe}(\text{OAc})_2$  concentrations obtained from two ideal trend (Indifferent and Pure Additive) and from experimental results (Experimental).

Figure 2 shows three linear trends that illustrate the relationship between the concentration of  $\text{Fe}(\text{OAc})_2$  added to the feedstock and the resulting solid residue yield after pyrolysis. The blue line represents the experimental results obtained from pyrolyzing the material at four different concentrations of iron acetate. The black line (Indifferent) shows the ideal trend based on the assumptions that 100 % of the iron acetate added to the feedstock remained in the pyro-char after pyrolysis and that PSW and Iron acetate pyrolyze purely additively (i.e. as there was no synergy between them) during pyrolysis. The values are calculated using Eq(1), where  $y_{100\%}$  represents the total pyro-char yield, calculated as the weighted sum of the solid  $\text{Fe}(\text{OAc})_2$  alone multiplied

by its concentration ( $x$ ) and  $y_{PSW}$  represents the yield in pyro-char from non-impregnated PSW multiplied by the complementing fraction. The red line (Pure Additive) plotted from values obtained with Eq(2), again assumes additive behavior, however this time the solid yield from  $\text{Fe}(\text{OAc})_2$  is set to 38 %, a value derived from pyrolysis of iron acetate alone under the same conditions described in the methods section.

$$y_{100\%} = 100\% \cdot x + y_{PSW} \cdot (1 - x) \quad (1)$$

$$y_{38\%} = 38\% \cdot x + y_{PSW} \cdot (1 - x) \quad (2)$$

All three lines have the same origin as it is the yield from the non-impregnated PSW ( $y_{PSW}$ ), and all of them are showing an upward trend. However, the slope of the Indifferent line indicates the highest yields This is based on the assumption that full retention of  $\text{Fe}(\text{OAc})_2$  in the pyro-char (100 %) occurs, meaning that all the iron acetate initially added to the feedstock remains entirely in the solid residue after pyrolysis. This, combined with the assumption of additive behavior between PSW and  $\text{Fe}(\text{OAc})_2$  leads to the highest calculated yields. In contrast, the Pure Additive line assumes partial retention, where only 38 % of the initial  $\text{Fe}(\text{OAc})_2$  is retained in the pyro-char, while the remaining is presumed to volatilize or decompose into non-solid products during pyrolysis. This results in intermediate yields compared to the Indifferent line. In reality, the role of iron during pyrolysis is very difficult to understand, since Iron is expected to react with carbon, oxygen and other metals to form oxides, carbides and alloys that are difficult to resolve in the typically complex heterogeneous chemical environment during pyrolysis. Notwithstanding such challenges, we know that Iron can catalyze the cracking of some precursors in the heterogeneous vapor/solid phase, leading to lower pyro-char yields. at the same time the formation of stable compounds, such as the aforementioned carbides or oxides would lead to an increase in the pyro-char yield. Accordingly, our results show an increase in solid yield with increasing concentration of iron acetate albeit with in lower values compared to the theoretical Pure Additive behavior. SEM micrographs (Figure 3) help to shed light on the thermochemical pathways involving iron.

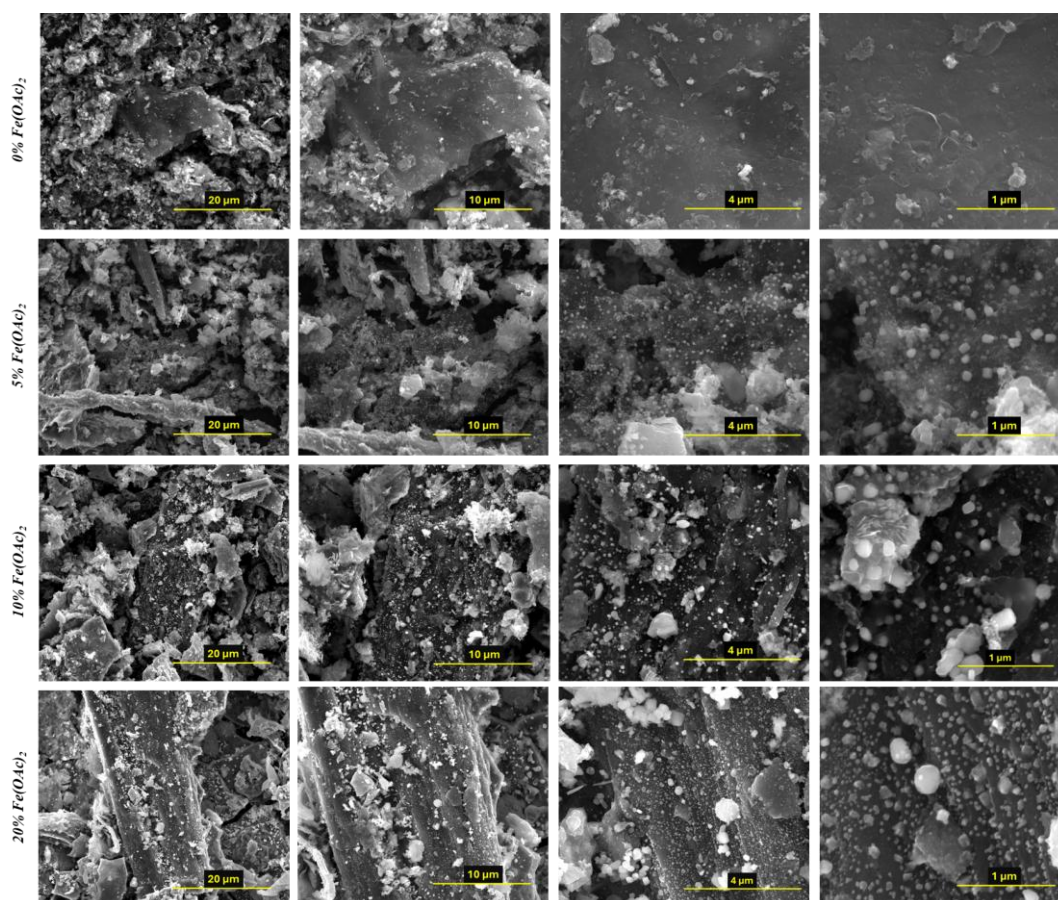


Figure 3: SEM micrographs of pyro-char at different  $\text{Fe}(\text{OAc})_2$  concentrations.

Figure 3 collects images taken at different magnifications and concentrations of  $\text{Fe}(\text{OAc})_2$ . In detail, the images are captured at an increase in magnification from left to right, while the salt concentration increases from top to bottom. The material appears heterogeneous in each image; however, the formation of white agglomerates was observed when pyro-char derived from an impregnated feedstock, while such agglomerations are not present in non-impregnated PSW (0 % w/w  $\text{Fe}(\text{OAc})_2$ ). While more in depth observations such as through transmission electron microscopy or x-ray diffraction is currently planned to gather more insights, the present images appear to show that such agglomerates derive by an interaction between iron and PSW during pyrolysis. The dimensions of these particles range between 20 and 200 nm suggesting potential sintering during the thermal process that we are currently further investigating through the preparation of samples under different (lower and higher) pyrolysis temperatures. Meanwhile, EDS on the pyro-char produced from the sample impregnated with 20 % w/w of  $\text{Fe}(\text{OAc})_2$  (Figure 4) are useful to observe the distribution of carbon, oxygen and iron to gather further insights (Figure 5).

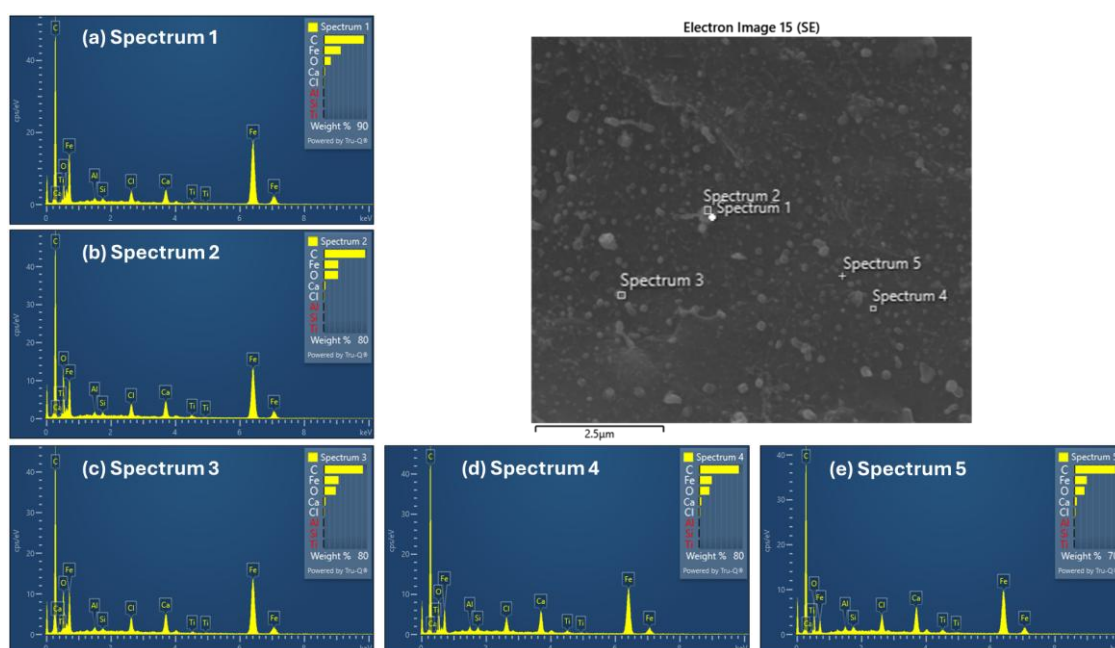


Figure 4: EDS point analysis of pyro-char produced from PSW and Iron Acetate at 20 % w/w.

Spectra obtained from single points (a and e) and from rectangular regions (b, c and d) all collected in correspondence of randomly selected agglomerations confirmed the presence of carbon, iron and oxygen, with traces of calcium and chlorine.

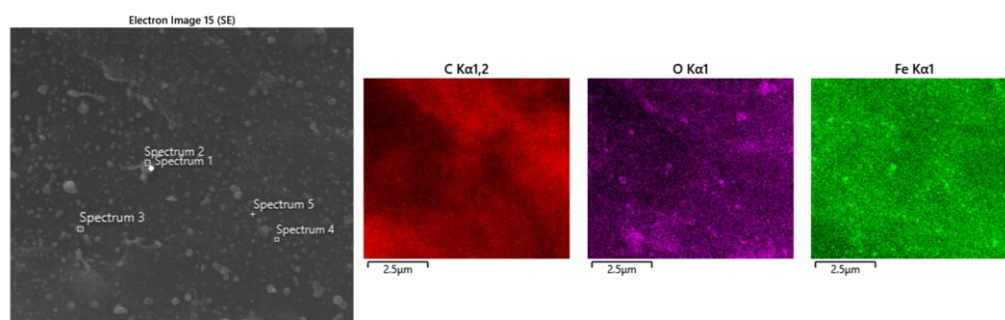


Figure 5: EDS map analysis of pyro-char produced from PSW and Iron Acetate at 20 % w/w.

On the other hand, a map of those elements on the entire region observed (Figure 5), shows a rather homogeneous distribution of those elements where iron appears at higher concentrations (brighter color) in small areas corresponding to the aforementioned agglomerates.

#### 4. Conclusions

The management of PSW is one of the ever-increasing environmental concerns, urging the need for sustainable solutions to its production use and disposal. The production of potentially valuable compounds *via* pyrolysis of plastic, opens a promising avenue. Importantly, transition metals, such as widely available and inexpensive iron can improve the yield and quality of pyrolysis products. This study focused on the effects of adding iron acetate on the properties of pyro-char derived from PSW, showing an increase in yield of pyro-char with increased concentration of iron acetate, yet also showing the complexity of some of the chemical transformations resulting from the process. The heterogeneity of waste feedstock and the many possible thermochemical pathways involving iron and the solid hydrocarbon can be observed by combined SEM and EDS analyses as a quick route to show the pathways to formation of iron-carbon-oxygen compounds. While more analysis is currently underway in our group, the present results show promising leads towards a facile upgrade of PSW in synergy with Iron, a route with significant potential to resolve the environmental hurdles currently affecting the conversion and disposal of plastic waste.

#### References

- Alanazi N.M., Adam F.M., Nagu M., 2017, Organochloride contamination in a refinery naphtha hydrotreater unit, *Materials Performance*, 56(10), 1-5.
- Al-Salem S.M., Antelava A., Constantinou A., Manos G., Dutta A., 2017, A review on thermal and catalytic pyrolysis of plastic solid waste (PSW), *Journal of Environmental Management*, 197, 177-198.
- Akhtar J., Saidina Amin N., 2012, A review on operating parameters for optimum liquid oil yield in biomass pyrolysis, *Renewable and Sustainable Energy Reviews*, 16(7), 5101-5109.
- Collard F.-X., Blin J., Bensakhria A., Valette J., 2012, Influence of impregnated metal on the pyrolysis conversion of biomass constituents, *Journal of Analytical and Applied Pyrolysis*, 95, 213-226.
- Ji M., Chen L., Que J., Zheng L., Chen Z., Wu Z., 2020, Effects of transition metal oxides on pyrolysis properties of PVC, *Process Safety and Environmental Protection*, 140, 211-220.
- Kylar mack, 2023, 65 Metals and Alloys Ranked by Cost Per Ounce <kylarmack.com/blogs/news/65-metals-and-alloys-ranked-by-cost-per-ounce> accessed 10.12.2024.
- Malik W., Tafoya J.P.V., Doszczeczko S., Sobrido J., Skoulou V.K., Boa A.N., Zhang Q., Ramirez Reina T., Volpe R., 2023, Synthesis of a graphene-encapsulated Fe<sub>3</sub>C/Fe catalyst supported on sporopollenin exine capsules and its use for the reverse water–gas shift reaction, *ACS Sustainable Chemistry & Engineering*, 11(44), 15795-15807.
- Marchetti L., Guastaferrero M., Annunzi F., Tognotti L., Nicoletta C., Vaccari M., 2024, Two-stage thermal pyrolysis of plastic solid waste: Set-up and operative conditions investigation for gaseous fuel production, *Waste Management*, 179, 77-86.
- Monlau F., Francavilla M., Sambusiti C., Antoniou N., Solhy A., Libutti A., Zabaniotou A., Barakat A., Monteleone M., 2016, Toward a functional integration of anaerobic digestion and pyrolysis for a sustainable resource management. Comparison between solid-digestate and its derived pyrochar as soil amendment, *Applied Energy*, 169, 652-662.
- Taghavi N., Abeykoon Udugama I., Zhuang W.-Q., Baroutian S., 2021, Challenges in biodegradation of non-degradable thermoplastic waste: from environmental impact to operational readiness, *Biotechnology Advances*, 49, 107731.
- Xia S., Yang H., Lei S., Lu W., Cai N., Xiao H., Chen Y., Chen H., 2023, Iron salt catalytic pyrolysis of biomass: Influence of iron salt type, *Energy*, 262, 125415.